ACS Macro Letters

Letter

pubs.acs.org/macroletters

Nucleation and Growth of Ordered Copolymer Structures at Reactive Interfaces between PA6 and MA-*g*-HDPE

Chloé Épinat,[†] Lise Trouillet-Fonti,[†] Stéphane Jéol,[‡] Didier R. Long,[†] and Paul Sotta*[,†]

[†]Laboratoire Polymères et Matériaux Avancés, CNRS/Rhodia-Solvay, UMR5268, 87 avenue des Frères Perret, Saint Fons Cedex 69192, France

[‡]Solvay R&I, 85 avenue des Frères Perret, Saint Fons Cedex 69192, France

ABSTRACT: We have studied the effect of the interfacial chemical reaction between PA6 and MA-*g*-HDPE in static conditions at a macroscopically flat interface. Interface destabilization and the growth of instabilities, somehow similar to myelin figures observed in surfactants put in the presence of water, are observed. For the first time in this system, it is shown that ordered microphase-separated copolymer domains, whose morphologies depend on the architecture of the copolymer, namely, essentially on the relative length of the blocks on each side of the interface, may nucleate and grow at a static interface between reactive polymers. We discuss the stability of the plane interface in the case of nonsymmetrical formed graft copolymers. The density of copolymers in the interface (coverage) can be estimated accurately from the long period of the formed structures. We confirm the predictions of Berezkin et al. This observation is very important since it confirms that nanometric domains are certainly generated during reactive extrusion, in addition to micrometric domains formed by rheological processes.

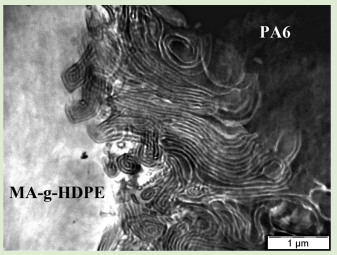

When processing compatibilized polymer blends by reactive extrusion, interface instabilities due to grafting chemical reactions at interfaces may coexist with rheology-driven mechanisms of domain breakup and coalescence under shear.[1] Discriminating both mechanisms may be a key issue in polymer science and engineering in order to better control the process and the obtained morphologies and therefore the properties of final products.[2]

When two reactive polymers react at a planar interface upon heating in static conditions, the formed copolymers accumulate at the interface, thus decreasing the interfacial tension and promoting interface fluctuations.[3−5] This leads to interfacial roughening, as was described in several polymer blends.[6−12] The kinetics is complex due to the stretching free energy barrier a chain has to overcome to reach the interface.[13−15] After interfacial roughening induced by fluctuations, emulsification and/or formation of micelles[6,11,12,16] or lamellae[7] have been observed. Recently, the coupling between immiscible polymers leading to the creation of block and graft copolymers of different architectures and the associated microstructure development was studied by mesoscale numerical simulations.[17−19]

This work is focused on the effect of the chemical reaction which happens at the interface in static conditions. We show new experimental results on the effect of the architecture of the formed copolymer and the subsequent destabilization of the interface and generation of ordered microphases, such as lamellar and cylindrical phases, from the interface. Our results offer the first direct experimental confirmation of the numerical predictions by Berezkin et al.[17−19]

We have used maleic anhydride-grafted high density polyethylene (MA-*g*-HDPE, M_n = 29 kg/mol, index of polydispersity 2.9) with 1 wt % of MA moieties (corresponding to an average of 2.9 MA groups per chain). Four linear polyamides 6 (PA6) of various chain lengths were synthesized: PA6−3k (M_n = 2.9 kg/mol, M_w = 6.6 kg/mol); PA6−10k (M_n = 11.2 kg/mol, M_w = 20.0 kg/mol); PA6−18k (M_n = 18.0 kg/mol, M_w = 37.0 kg/mol); PA6−31k (M_n = 30.5 kg/mol, M_w = 59.4 kg/mol). Molecular masses are from GPC analysis. M_n values from GPC are coherent with those measured by end group titration.[21] In reactive blending, MA groups react with the NH_2 end group of PA6.[20] Dried films (20−100 μm thick) of each polymer were first prepared by compression molding. For each PA6, MA-*g*-HDPE, and PA6 alternated stacks were prepared, pressed together in a hermetic cell with argon atmosphere and inserted for various durations (10−70 min) in a preheated oven at 290 °C (thermalization of the whole cell takes about 8 min). Samples were then quenched down to room temperature by cold nitrogen gas flow. Ultrathin (80 nm) sections were cryomicrotomed perpendicularly to initial interfaces, stained with phosphotungstic acid, and observed by TEM (Figure 1).

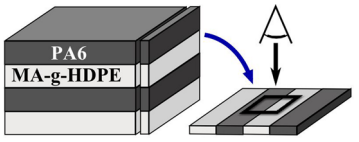

Figure 1. Schematics of interface observation in annealed PA6/MA-*g*-HDPE stacks.

Received: February 20, 2015
Accepted: April 13, 2015
Published: April 14, 2015

DOI: 10.1021/acsmacrolett.5b00139
ACS Macro Lett. 2015, 4, 488−491

As a preliminary observation, interfaces between PA and PE films remain flat and nonadhesive when nonreactive HDPE was used instead of MA-*g*-HDPE. The same was observed when MA-*g*-HDPE was used, but the samples were heated to 160 °C only, that is, when only the PE part melted, which prevents the interfacial reaction to occur, except perhaps for a few PA chains which happen to be in direct contact with the interface (Figure 2(a)).

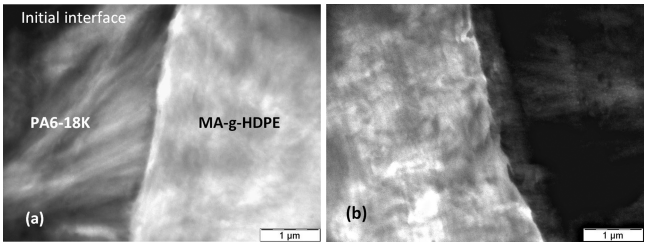

Figure 2. Interface in (a) MA-*g*-HDPE/PA6−18k pressed at 160 °C for 10 min (no reaction occurred) and (b) MA-*g*-HDPE/PA6−3k annealed at 290 °C during 70 min. The PA6 phase appears as dark.

After annealing at 290 °C, no roughening or morphology development was observed for sandwiches with PA6−3k. Interfaces remained flat (Figure 2(b)). Nevertheless, in contrast to the nonreactive cases, strong adhesion between adjacent PA and PE layers was noticed when preparing thin samples for TEM observation. This can be considered as indirect proof that a coupling reaction indeed occurred at the interface. Note that some very rare, isolated PA6 droplets of diameter of the order 200 nm that stuck to the otherwise flat interface start to appear after 25 min.

In sandwiches with the three other PA6's (PA6−10k, PA6−18k, and PA6−31k), interfaces destabilize within less than 10 min upon static annealing at 290 °C. Initially flat interfaces proliferate, leading to large-scale interfacial roughening, as already described in other systems.[6−12] In order to distinguish the structures which develop and discuss underlying mechanisms, one then needs to look at small scales. In all three cases, nucleations of local structures, cylinders or lamellae, are observed. Some domains grow into locally ordered mesophase morphologies.

For PA6−10k samples (Figure 3), the overall thickness of the roughened interface is of the order 500 nm−1 μm after 10 min

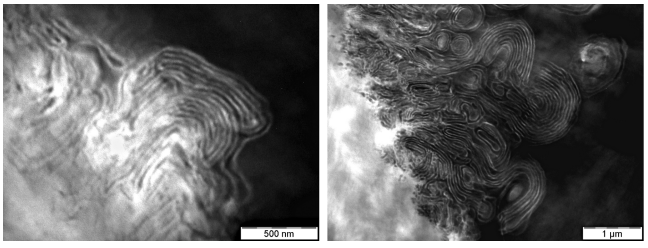

Figure 3. Morphology developed at the MA-*g*-HDPE/PA6−10k interface after annealing at 290 °C during 10 min (left) and 70 min (right). The PA6 phase appears as dark.

annealing and reaches 2−3 μm after 60 min. Closer inspection shows that the morphology which develops mostly consists of tubes or filaments made of concentric cylinders, indicating that the structure is locally lamellar. These tubes seem to grow at a given angle (close to perpendicular) with respect to the initial flat interface and fold in worm-like structures as they develop further. The cylinders/filaments evolve into or coexist with droplets of the PA phase inside the PE phase. These cylinders may be reminiscent of focal conic domains observed in smectic liquid crystals[22] as well as of myelin figures observed when a concentrated surfactant solution is put in the presence of water,[23−27] which provides a strong, indirect indication that the structure is indeed locally lamellar. The apparent period of the lamellar array, of the order 32.5 nm, and apparent thickness of PA layers, of the order 17.5 nm, stay roughly constant throughout annealing (even though it perhaps increases a little).

There is a gradient of morphologies throughout the whole interfacial area, going from a foam-like PE phase with PA droplets on the PE side toward well-formed lamellar packings on the PA side.

PA6−18k samples show quite symmetrical patterns (Figure 4), with both PA filaments in the PE phase and PE filaments in

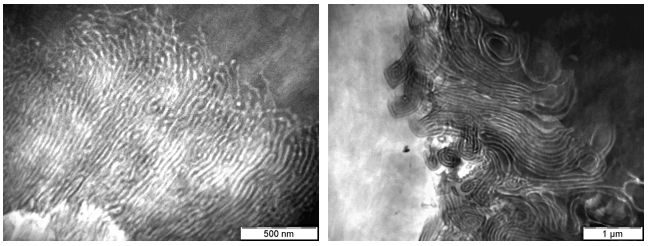

Figure 4. MA-*g*-HDPE/PA6−18k interface after annealing at 290 °C during 10 min (left) and 70 min (right). The PA6 phase appears as dark.

the PA phase, both initiating perpendicular to the initial locally flat interface and evolving into a locally lamellar structure forming worm-like tubes as in the PA6−10k samples. The apparent period, roughly constant along annealing, is of the order 37−40 nm, i.e. consistently a little longer than in the 10k case. The diameter of PE filaments inside the PA phase is of the order 16.5−17 nm. Growth is a little faster than in the 10k case, with an overall interface thickness of about 1.5 μm after 10 min annealing.

In PA−31k samples, filaments of PA grow preferentially into the PE phase (Figure 5). Growth is slower than in PA6−18k

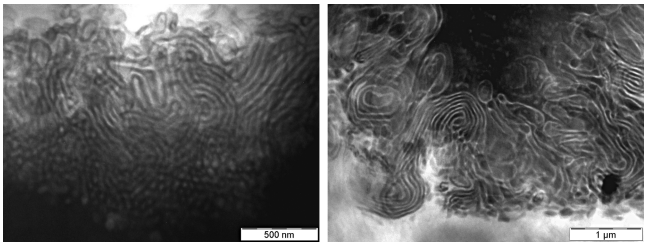

Figure 5. MA-*g*-HDPE/PA6-31k interface after annealing at 290 °C during 10 min (left) and 70 min (right). The PA6 phase appears as dark.

samples. When compared to PA6−10k samples, some clear phase inversion-like phenomenon appears: while PA6−10k samples exhibit preferentially PA droplets (or sections of cylinders) within the PE phase, PA6−31k samples show preferentially PE droplets (or isolated filaments) within the PA

DOI: 10.1021/acsmacrolett.5b00139
ACS Macro Lett. 2015, 4, 488−491

phase. The apparent period of arrays is of the order 47.5−50 nm.

Let us now discuss the results, which may be summarized as follows: the formed structures (micelles, cylinders, lamellae) depend on block length; growth occurs at a defined angle with respect to the initial flat interface; the kinetics is faster in the lamellar case; the long periods of the observed arrays are compatible with those of structures observed in pure block copolymers at equilibrium in the strong segregation regime.[28] The apparent long period goes from about 32.5 nm (PA6−3k) to 47 nm (PA6-31k). It agrees qualitatively with the variation of chain length. Data are not quantitative enough to check a possible power law variation of the period as a function of the average chain length. The apparent long period of the microphase-separated domains does not vary significantly with the annealing time (even though it perhaps increases a little). This indicates that structures are nucleated with a copolymer density at the interface (coverage) already close to the final, equilibrium value. Samples with PA6−18k exhibit both the most symmetric (namely, lamellar) morphologies at the three tested annealing times and the fastest growth. Also, a gradual change of microstructure is observed perpendicular to the initial interface. At some point, micelles or cylinders formed at the basis of the interface evolve into lamellae, for example. This gradual change most probably results from a gradient of concentration within the interfacial region.

The copolymer density within the interface (coverage) may be estimated from the value of the long period. Let us assume that interfaces are completely filled by copolymers ("dry brush" approximation). For PA6−10k, assuming that PA lamellae have a thickness $D \approx 20$ nm and denoting a^2 the average area per chain, the volume occupied by a chain is Da^2, which, when equated to the number-average chain volume $v_c = M_n/(N_a\rho)$ (where M_n is in kg/mol, N_a is Avogadro's number, and the density ρ is of the order 10^3 kg/m^3), gives $a^2 = v_c/D \approx 7.6$ nm^2 or equivalently, an interfacial coverage (number of PA chains per unit area) $a^{-2} = 0.13$ chain/nm^2. This value is of the same order as those estimated in other systems.[9,30]

In block copolymers, the microphase-separated structures depend on the spontaneous curvature of the interfaces, determined by the relative length of segregated blocks.[31] The observed microphase structures indeed depend on the PA chain length. However, this dependence is not very sensitive, essentially because chain length distributions of our various PA samples overlap quite largely. A criterium for obtaining lamellar structure (zero average curvature) at equilibrium has been proposed for linear diblock copolymers[31] and further extended to star-block copolymers. Assuming that the graft copolymer formed here behaves in the same way as a Y-shaped copolymer, with a PA block and two PE arms attached to it, this criterium would write $V_A^3/R_{GA}^2 = 2^4 V_B^3/R_{GB}^2$,[32,33] where V_i is the molecular volume of the i block and R_{Gi} its radius of gyration, and index A stands for the PA block and B for PE arms. On the basis of the M_n value of each PA sample, the predicted equilibrium morphologies would be formed of PA micelles for the PA6−3k sample, PA cylinders for PA6−10k, and lamellae for PA6−18k and PA6−31k.

The proposed mechanism is schematized in Figure 6. Since lamellae or cylinders grow perpendicular, or at a nonzero angle with respect to the initially flat interface, unreacted polymers on each side can diffuse along lamellae (or cylinders) toward the interface, without having to overcome very high free energy barriers associated with crossing through lamellae. The growth mechanism is then kinetically limited by diffusion of unreacted chains along lamellae or cylinders.

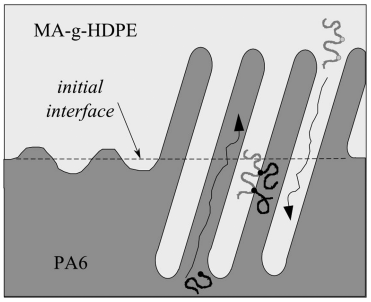

Figure 6. Schematics of the proposed lamella growth mechanism based on observation. Interface instabilities give rise to nucleation and growth of locally ordered copolymer structure.

All these observations are in remarkable agreement with the predictions by Berezkin et al. obtained by dissipative particle dynamics (DPD) simulations.[17−19] Also in agreement with theoretical predictions and simulations is the observed strong slowing down of the kinetics during annealing, related to the increasingly high stretching free energy barrier that chains have to overcome to reach the interface and react.[3,14,15,29] Also, it is observed qualitatively that the kinetics is consistently slower for longer chains.

One specific result observed here is that interfaces do not destabilize for the PA6−3k sample. This can be explained as follows. Block copolymers accumulating at an interface decrease the surface tension until saturation of the copolymer brush is reached when block stretching on each side balances the excess contact energy.[34] In PA6−3k samples, since PA chains (blocks) are much shorter than PE blocks, brush saturation is reached for PE blocks, while PA blocks are still far from saturation. Therefore, there is no significant reduction of surface tension due to chain stretching on the PA side of the flat interface. The overall minimum of interfacial tension would correspond to a nonzero equilibrium curvature of the interface, toward the shorter block side. However, the flat interface does correspond to a metastable state. Indeed, for an interface with (spontaneous) curvature C_0 at equilibrium, the excess energy per unit plane surface area associated with a deviation u from the plane interface is $\Delta F(u) = \int[((\gamma/2)q^2 + (\kappa/2)q^4)u(q)u(-q) - \kappa C_0 u(q)]\mathrm{d}^2q$, where $u(q)$ is the mode of wave vector q (within the plane of the interface). The first term is associated with the excess area created by fluctuations and the second term with curvature energy. γ is the surface tension and κ the elastic constant for curvature. For $C_0 \neq 0$, a plane interface ($u(q) = 0$) does not correspond to the most stable state of the interface. However, the $\Delta F(u)$ curve is concave at the point $u(q) = 0$ (corresponding to plane interface), which means that any fluctuation shall increase the free energy, thus corresponding to metastability.

The fact that PA6−3k does not exhibit interface destabilization, even though block diffusion toward the interface should be faster in this case, indicates that reaching brush saturation on both sides is a key prerequisite for interface destabilization and subsequent growth of morphologies.

Then, to generate a micelle of radius R from the initially flat interface, an extra area $4\pi R^2$ must be created, which corresponds to an excess interface energy $4\pi\gamma R^2$. Taking γ to be half the raw HDPE/PA6 surface tension, $\gamma_0 \approx 1.2 \times 10^{-2}$ N m^{-1} in the PA6−3k case[35] gives $\gamma \approx 6 \times 10^{-3}$ N m^{-1}. With $R \approx$

DOI: 10.1021/acsmacrolett.5b00139
ACS Macro Lett. 2015, 4, 488−491

10 nm, $4\pi\gamma R^2 \approx 7.5 \times 10^{-18}$ J $\approx 10^3 k_B T$ at $T \approx 290$ °C. This illustrates how much it costs to increase the interface area (as soon as $\gamma \neq 0$) and shows that generating a micelle from the interface is impossible in static conditions.

In conclusion, for the first time, the nucleation and growth of ordered microphase-separated copolymer domains at flat polyamide/polyethylene interfaces, due to chemical reaction between reactive immiscible blocks under static conditions, has been described. For long chains, instabilities, somehow similar to myelin figures observed in surfactants put in the presence of water, develop, whereas interfaces with shorter PA6 chains remain metastable. This indicates that, at the considered temperature, the density of graft copolymers at the interface (interface coverage) can reach values that are beyond saturation, thus leading to interface destabilization.

The architecture of the copolymer created at the interface affects not only the initiation of interfacial fluctuations but also the microstructures which are formed as a result of interface destabilization. These microstructures are similar to those observed in block copolymers and thus depend on the relative length of the blocks on each side of the interface. Indeed this ratio of lengths determines the local equilibrium curvature of the interface. We confirm the predictions of Berezkin et al.[17] This observation is very important since it confirms that nanometric domains may be formed during reactive extrusion, in addition to purely rheological processes, like Taylor drop breakup[36] and coalescence and/or Plateau−Rayleigh instability of elongated threads,[1] which lead to micrometric domain formation.

AUTHOR INFORMATION

Corresponding Author

*E-mail: paul.sotta-exterieur@solvay.com.

Notes

The authors declare no competing financial interest.

ACKNOWLEDGMENTS

We thank LSPP laboratory for helping in the synthesis of PA6 materials and the GPC and microscopy laboratories at Solvay R&I Center Lyon.

REFERENCES

(1) Meijer, H. E. H., Janssen, J. M. H., Anderson, P. D. *Mixing and Compounding of Polymers, Theory and practice*, 2nd ed.; Carl Hanser Verlag: Munchen, 2009; pp 1−147.

(2) Pernot, H.; Baumert, M.; Court, F.; Leibler, L. *Nat. Mater.* **2002**, *1*, 54−58.

(3) Fredrickson, G. H.; Milner, S. T. *Macromolecules* **1996**, *29*, 7386−7390.

(4) Shull, K. R.; Kramer, E. J.; Hadziiannou, G.; Tang, W. *Macromolecules* **1990**, *23*, 4780−4787.

(5) Shull, K. R.; Kellock, A.; Deline, V.; MacDonald, S. *J. Chem. Phys.* **1992**, *97*, 2095−2104.

(6) Zhang, C. L.; Lodge, T. P.; Macosko, C. W. *Macromolecules* **2005**, *38*, 6586−6591.

(7) Lyu, S. P.; Cernohous, J. J.; Bates, F. S.; Macosko, C. W. *Macromolecules* **1999**, *32*, 106−110.

(8) Schulze, J. S.; Cernohous, J. J.; Hirao, A.; Lodge, T. P.; Macosko, C. W. *Macromolecules* **2000**, *33*, 1191−1198.

(9) Yin, Z.; Koulic, C.; Pagnoulle, C.; Jérôme, R. *Langmuir* **2003**, *19*, 453−457.

(10) Jiao, J.; Kramer, E. J.; De Vos, S.; Müller, M.; Koning, C. *Polymer* **1999**, *40*, 3585−3588.

(11) Kim, H. Y.; Jeong, U.; Kim, J. K. *Macromolecules* **2003**, *36*, 1594−1602.

(12) Kim, J. K.; Kang, H.; Char, K.; Katsov, K.; Fredrickson, G. H.; Kramer, E. J. *Macromolecules* **2005**, *38*, 6106−6114.

(13) Ligoure, C.; Leibler, L. *J. Phys.* **1990**, *51*, 1313−1328.

(14) O'Shaughnessy, B.; Sawhney, U. *Macromolecules* **1996**, *29*, 7230−7239.

(15) O'Shaughnessy, B.; Vavylonis, D. *Macromolecules* **1999**, *32*, 1785−1796.

(16) Bhadane, P. A.; Tsou, A. H.; Cheng, J.; Favis, B. D. *Macromolecules* **2008**, *41*, 7549−7559.

(17) Berezkin, A. V.; Kudryavtsev, Y. V. *Macromolecules* **2011**, *44*, 112−121.

(18) Berezkin, A. V.; Guseva, D.; Kudryavtsev, Y. *Macromolecules* **2012**, *45*, 8910−8920.

(19) Berezkin, A. V.; Kudryavtsev, Y. V. *Macromolecules* **2013**, *46*, 5080−5089.

(20) Argoud, A.; Trouillet-Fonti, L.; Ceccia, S.; Sotta, P. *Eur. Polym. J.* **2014**, *50*, 177−189.

(21) Note that a small residual fraction of cyclic oligomers is present in PA6.

(22) Kleman, M. *Points, Lines and Walls in Liquid Crystals, Magnetic Systems and Various Ordered Media*; John Wiley and Sons: New York, 1982.

(23) Buchanan, M.; Arrault, J.; Cates, M. *Langmuir* **1998**, *14*, 7371−7377.

(24) Buchanan, M.; Egelhaaf, S.; Cates, M. *Langmuir* **2000**, *16*, 3718−3726.

(25) Haran, M.; Chowdhury, A.; Manohar, C.; Bellare, J. *Colloids Surf., A* **2002**, *205*, 21−30.

(26) Reissig, L.; Fairhurst, D.; Leng, J.; Cates, M.; Mount, A.; Egelhaaf, S. *Langmuir* **2010**, *26*, 15192−15199.

(27) Zou, L.-N. *Phys. Rev. E* **2009**, *79*, 061502.

(28) Hamley, I. W. *The Physics of Block Copolymers*; Oxford University Press: New York, 1998.

(29) Fredrickson, G. H. *Phys. Rev. Lett.* **1996**, *76*, 3440−3443.

(30) Jeon, H. K.; Macosko, C. W.; Moon, B.; Hoye, T. R.; Yin, Z. *Macromolecules* **2004**, *37*, 2563−2571.

(31) Leibler, L. *Makromol. Chem., Macromol. Symp.* **1988**, *16*, 1−17.

(32) Milner, S. T. *Macromolecules* **1994**, *27*, 2333−2335.

(33) Lee, C.; Gido, S. P.; Poulos, Y.; Hadjichristidis, N.; Beck Tan, N.; Trevino, S. F.; Mays, W. *Polymer* **1997**, *39*, 4631−4638.

(34) Ohta, T.; Kawasaki, K. *Macromolecules* **1986**, *19*, 2621−2632.

(35) Minkova, L.; Yordanov, Hr.; Filippi, S.; Grizzuti, N. *Polymer* **2003**, *44*, 7925−7932.

(36) Taylor, G. I. *Proc. R. Soc. London A* **1932**, *138*, 41−48.

DOI: 10.1021/acsmacrolett.5b00139
ACS Macro Lett. 2015, 4, 488−491